Electrical transport through $Pb(Zr,Ti)O_3$ *p-n* and *p-p* heterostructures modulated by bound charges at a ferroelectric surface: Ferroelectric *p-n* diode

Yukio Watanabe
Kyushu Institute of Technology, Tobata, Kitakyushu 804, Japan
(Received 23 January 1998; revised manuscript received 8 July 1998)

Current through $(Pb,La)(Zr,Ti)O_3$ ferroelectrics on perovskite semiconductors is found to exhibit diode characteristics of which polarity is universally determined by the carrier conduction-type semiconductors. A persisting highly reproducible resistance modulation by a dc voltage, which has a short retention, is observed and is ascribed to a band bending of the ferroelectric by the formation of charged traps. This interpretation is consistent with a large relaxation current observed at a low voltage. On the other hand, a reproducible resistance modulation by a pulse voltage, which has a long retention, is observed in metal/$(Pb,La)(Zr,Ti)O_3$/$SrTiO_3$:Nb but not in metal/$(Pb,La)(Zr,Ti)O_3$/$(La,Sr)_2CuO_4$ and is attributed to a possible band bending due to the spontaneous polarization (P) switching. The observed current voltage (IV) characteristics, the polarity dependence, the relaxation, and the modulation are explicable, if we assume a *p-n* or a *p-p* junction at the ferroelectric semiconductor interface (*p*: hole conduction type, *n*: electron conduction type). The analysis suggests that an intrinsically inhomogeneous P (∇P) near the ferroelectric/metal interface is likely very weak or existing in a very thin layer, when a reaction of the metal with the ferroelectric is eliminated. Additionally, the various aspects of transport through ferroelectrics are explained as a transport in the carrier depleted region. [S0163-1829(99)09917-8]

I. INTRODUCTION

Electrical properties of ferroelectric are known to be closely connected with its crystallographic structure. Nonetheless, the free carriers play an essential part in determining ferroelectric properties of some narrow band-gap materials.[1] Additionally, a few studies suggest that the free carriers at the surface stabilize the ferroelectric phase and that a degenerate electron gas is formed at an ideal surface.[2–4] However, there have not been many experimental reports on the interaction of the free carrier with ferroelectric properties, especially the spontaneous polarization (P).[5,6]

The carrier transport through a ferroelectric reflects the interaction of free carriers with P and the band structure of the ferroelectric surface. In an ideal ferroelectric, the bound charges due to P appear only near the ferroelectric surface. Therefore the interaction is difficult to detect in bulk samples, in which the carrier transport is mainly determined by resistance of the bulk part or the grain boundaries.

The carrier transport across semiconductor surface is considered to be governed by the Schottky barrier and the *p-n* junction (*p*: hole conduction type, *n*: electron conduction type). Ideally, the Schottky barrier height is estimated from the metal work function and the electron affinity of the semiconductor as proposed by Schottky[7] and Mott.[8] Experimentally, the barrier heights deviate often from this estimate due to the surface states. Similarly, the formation of *p-n* heterojunction has been successful only for a limited number of semiconductors such as III-V and II-VI compounds so far. This is due to the difficulty of forming both *p*- and *n*-type using given semiconductors and the formation of surface states at the junction.[9] Viewing this differently, the significant effect of the surface states suggests a possible control of the barrier height or the built-in potential by surface bound charges Q, e.g., due to P.

Recently, a transport property related to this possibility was reported in epitaxial ferroelectric films.[10–13] The current through ferroelectric exhibit a diode property tunable by an external voltage bias. However, its origin has yet been unidentified, although two mechanisms, the charge injection and the P switching, were proposed. Moreover, the conduction mechanism in ferroelectric film which is a basis for understanding the origin, has been controversial. If this effect is due to a change of the metal/ferroelectric contact by P without surface dead layer in a ferroelectric,[12] these phenomena support the existence of a ∇P effect.[14]

The present article proposes an answer to these questions by a systematic study of the current voltage (IV) characteristics. By choosing the voltage and materials, we demonstrate a very reproducible IV, while the reproducibility and the repeatability are not addressed in Ref. 12. The diodelike IV characteristics exhibit a universal polarity dependence of the forward bias on perovskite electrodes previously reported partially by us.[15] Next, a dc voltage (V_{dc}) and persistent pulse voltage (V_{pulse}) modulations of a dc conduction are demonstrated. The results are explained using the band diagram.

II. EXPERIMENT

$Pb_{1-y}La_yZr_{1-x}Ti_xO_{3\pm\delta}$ ($x=0-0.5$, $y=0-0.15$) films were epitaxially grown by the pulse laser deposition on (100) $SrTiO_3$ doped with 0.5 weight % Nb (STON) as well as on $La_{1.99}Sr_{0.01}CuO_4$ (LCO), $Nd_{1.99}Ce_{0.01}CuO_4$ (NCO), and $LaNiO_3$ films formed on (100) $SrTiO_3$ (STO). $Pb_{1-y}La_yZr_{1-x}$ $Ti_xO_{3\pm\delta}$, LCO, and $LaNiO_3$ are *p*-type with carrier density of $10^{17}-10^{21}$ cm^{-3} at room temperature (RT), while STON and NCO are *n*-type. We abbreviate $Pb_{1-y}La_yZr_{1-x}Ti_xO_{3\pm\delta}$ with $x=0.3$ and $y=0.1$ as PLZT and concentrate on PLZT,[16] because similar results were obtained for other combinations of x and y. All the PLZT/LCO

and the PLZT/STON heterostructures in this article were deposited in the same batch. Details of the surface morphology, the crystallographic properties, and their deposition conditions are described elsewhere.[17] The oxide conductive layer, which serves as a bottom electrode, is 100 nm thick, and the ferroelectric layer is approximately 200 nm thick. The x-ray diffraction shows that all heterostructures are *c*-axis oriented with a strong diffraction intensity comparable to single crystals and all the layers are aligned in plane to the *a* axis of the substrate. No secondary phases are detected by the depth profile using Auger electron spectroscopy and x-ray diffractometry.

Au and Pt films with surface area of 0.2, 1, and 2.25 mm^2 were deposited on the heterostructures as top electrodes. The annealing of the metal electrodes, which is usually performed, are not carried out to minimize the reaction at the metal/ferroelectric interface. The remanent polarization Pr measured by Sawyer-Tower method is 3–7 $\mu C/cm^2$ at maximum applied voltage of 10 V at 1 kHz.[18] The current (I_L) was measured by applying a V_{dc} across a ferroelectric film, where its bottom conductive layer or its substrate was grounded. The V_{dc} was first increased from zero to the maximum ($+V_{max}$), then decreased to the minimum ($-V_{max}$) passing through zero, and finally returned to zero. One *IV* curve was measured in approximately 7 min, and each data point was obtained, waiting about 2 s after V_{dc} was applied. We confirmed that the qualitative features of *IV* characteristics were the same as below, even when the metal/PLZT contact area was reduced to $\sim 100\ \mu m^2$.[19]

The poling by a dc voltage accompanies inevitably a large amount of carrier injection, which obscures a possible conduction modulation by the *P* switching. By utilizing a short pulse and selecting its width and its height, we attempted to suppress the carrier injection, while still accomplishing the *P* switching, i.e., the domain-wall motion.

The following results are representative of many $Pb_{1-y}La_yZr_{1-x}Ti_xO_3$ heterostructures studied, e.g., 200 samples for measurements in Fig. 1 (see Appendix A). We measured the same position of a same sample for all the results below, unless otherwise stated.

III. RESULTS

Figure 1 shows typical *IV* characteristics of Au/PLZT/STON and Au/PLZT/LCO for various V_{max}. Each panel of Fig. 1 displays multiple *IV* curves consecutively measured, demonstrating the reproducibility.

For $V_{max}=0.2$ V [Figs. 1(a) and 1(d)], I_L exhibits hystereses symmetric with respect to V_{dc}. I_L at a given V_{dc} is smaller for decreasing $|V_{dc}|$ than for increasing $|V_{dc}|$ ($|V_{dc}|$: the absolute value of V_{dc}). Furthermore, the polarity of I_L is partly opposite to V_{dc}. These observations suggest that the hystereses are due to a relaxation of trapped carriers or a dielectric relaxation. The initial overshoot of I_L in Fig. 1(d) also supports this view. The large oscillations in Figs. 1(a), 1(b), and 1(d) are not instrumental but are likely due to the trapping/detrapping of the carriers at PLZT surfaces, because the oscillation amplitude decreases with repeated measurements. The oscillations have a quasiperiodicity, although it is obscured by overlapping of five *IV* curves in each panel. In

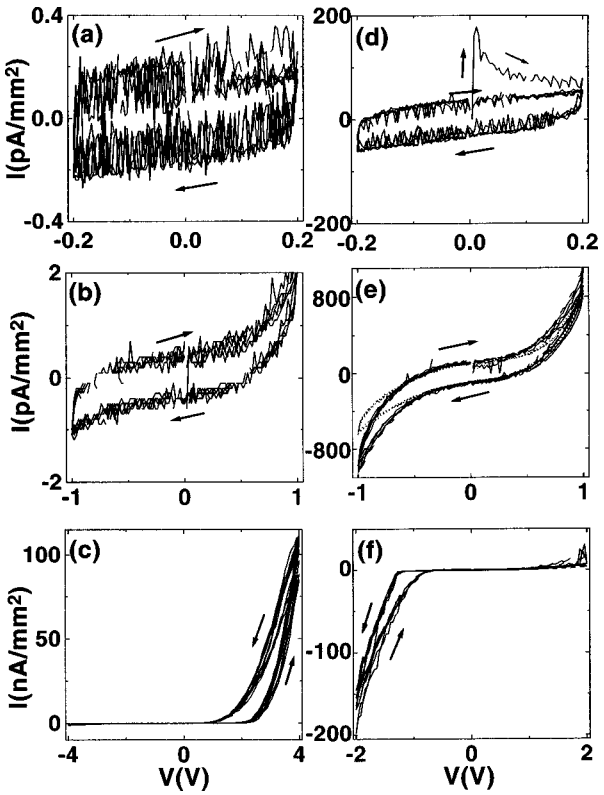

FIG. 1. *IV* curves for PLZT/STON [(a)–(c)] and PLZT/LCO [(d)–(f)] for different V_{max}'s. Each panel of (a)–(d), (c), and (f) show five, ten, and six *IV* curves consecutively measured, respectively. In (e), the *IV* curves before and after the measurement of the data in (f) are shown by the dashed and dotted lines, respectively.

samples with a low resistance, neither relaxation or oscillation at a low V_{dc} is detected.

As V_{max} increased, *IV* curves become nonlinear exhibiting still symmetric relaxation-dominated hystereses [Figs. 1(b) and 1(e)]. By increasing V_{max} further, diodelike *IV* characteristics emerge [Figs. 1(c) and 1(f)]. At the forward bias, reproducible resistance modulations, i.e., hystereses, are evident. Namely, I_L at a given V_{dc} is larger for decreasing $|V_{dc}|$ than for increasing $|V_{dc}|$. A sharp increase of I_L is evident at 2 V in Fig. 2(c) and at -1.3 V in Fig. 2(f), while these voltages corresponds approximately to the coercive field. The maximum resistance ratio of the resistive to the conductive state is 300 for the PLZT/STON and 20 for the PLZT/LCO. At the reverse bias, I_L at a given V is smaller for decreasing $|V_{dc}|$ than for increasing $|V_{dc}|$. This indicates that the hystereses at the reverse bias in Figs. 2(c) and 2(f) are due to a relaxation.

In Fig. 1, the forward bias is positive for the heterostructures with *n*-type bottom electrodes and negative for those with *p*-type bottom electrodes. Similar *IV* characteristics are observed when the top electrode is Pt. The current density at both forward and reverse biases is of order of magnitude the same in Au/PLZT/STON and Pt/PLZT/STON.[20] However, the current density at both forward and reverse biases is larger by a factor of 10^3 in Pt/PLZT/LCO than in Au/PLZT/LCO. These observations support that I_L is limited at the PLZT/STON interface in metal/PLZT/STON and at the metal/PLZT interface in metal/PLZT/LCO.

Dependence of the diode polarity on the bottom elec-

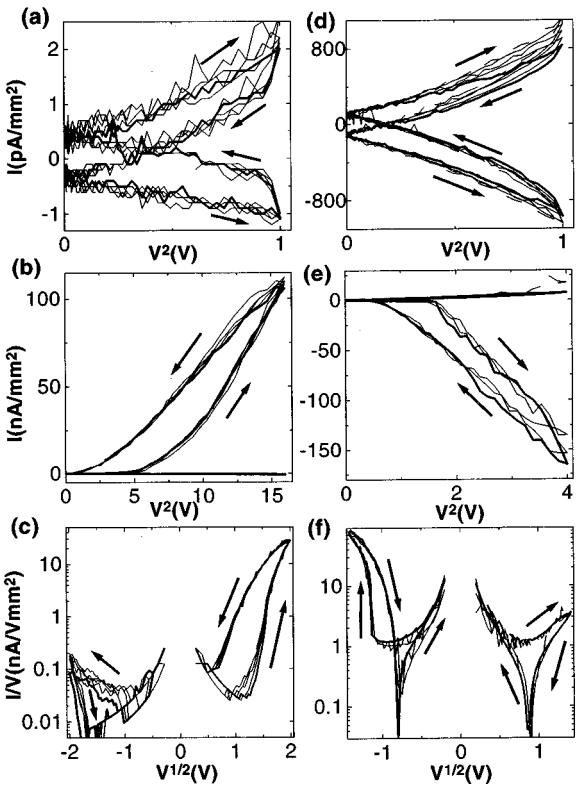

FIG. 2. Replots of *IV* curves in Fig. 1(b) [(a)], 1(c) [(b)], 1(e) [(d)], and 1(f) [(e)] in accordance with a SCL conduction model and *IV* curves in 1(c) [(c)] and 1(f) [(f)] in accordance with a PFL conduction model. Each panel shows five consecutive *IV* curves, while one representative curve is shown by a thick line.

trode similar to Fig. 1 is invariably observed in other heterostructures such as $Pb_{1-y}La_yZr_{1-x}Ti_xO_{3\pm\delta}$/LCO, $Pb_{1-y}La_yZr_{1-x}Ti_xO_{3\pm\delta}$/STON ($x=0.2$, 0.3, $y=0.05$, 0.10), $Pb_{0.95}La_{0.05}Zr_{0.2}Ti_{0.8}O_{3\pm\delta}$/NCO, $Pb_{1-y}La_yTiO_{3\pm\delta}$/LCO, $Pb_{1-y}La_yTiO_{3\pm\delta}$/$LaNiO_3$, $Pb_{1-y}La_yTiO_{3\pm\delta}$/STON ($y=0.05$, 0.10), $PbZr_{0.5}Ti_{0.5}O_{3\pm\delta}$/LCO, $PbZr_{0.5}Ti_{0.5}O_{3\pm\delta}$/$LaNiO_3$, $PbZr_{0.5}Ti_{0.5}O_{3\pm\delta}$/STON (Appendix A).[21]

After the *IV* curves for $V_{max}=2$ V were obtained, *IV* characteristics for $V_{max}=1$ V were measured again [dotted lines in Fig. 1(e)]. The *IV* characteristics before and after the resistance modulation [Fig. 1(f)] are almost the same. This observation and the reproducibly observed high resistance at the reverse bias in Fig. 1 elucidate that the resistance modulation is not a simple resistance degradation.

The stereotype conduction mechanisms for insulators are grossly classified as the thermionic emission limited (TEL), the Poole-Frenkel emission limited (PFL), the Fowler-Nordheim tunneling, and the space charge limited (SCL).[22] Figure 2 shows the replots of Fig. 1 that yield linear relationships, i.e., plots in the SCL and the PFL model. Little difference between the TEL and the PFL plot is found for $|V_{dc}|>0.5$ V. The SCL model appears to be appropriate for *IV* with a low V_{max} [Figs. 2(a) and 2(d)].

Figure 2 shows that the conduction mechanism is changed from a PFL/TEL to a SCL by a large forward V_{dc}. The carriers are likely injected into the interface that limits I_L, i.e., Au/PLZT in Au/PLZT/LCO or PLZT/STON in Au/PLZT/STON [Figs. 2(b) and 2(e)]. This would generate trap sites and facilitate a PFL/TFL transport, and the PFL/TFL transport would cease to limit the current. Therefore a transport in the entire carrier depleted region [depletion layer] of PLZT, which is the SCL, starts to limit I_L. In some other samples, the apparent conduction mechanism is different: only a SCL, or a PFL, or a TEL is observed, or the conduction mechanism changes gradually.

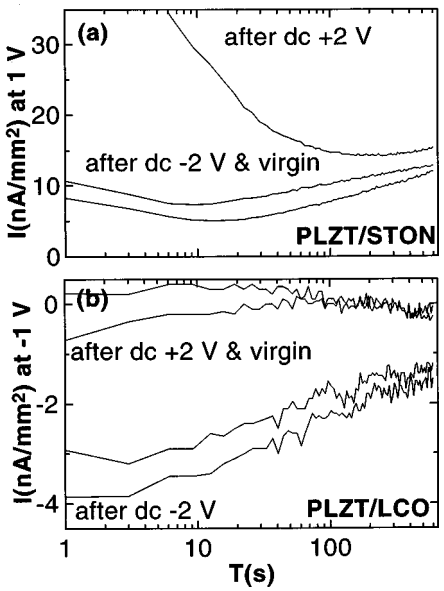

FIG. 3. *I-t* curves of Au/PLZT/STON (a) and Au/PLZT/LCO (b) after ± 2 V V_{dc}'s. The sample for (a) is different from that used in Figs. 1(a)–1(c). The sample for (b) is that used in Figs. 1(d)–1(f).

Figures 1(c) and 1(f) demonstrate a reproducible reduction of the resistance by a forward V_{dc} and its restoration to an original value by a reverse V_{dc}. Unlike *IV* hystereses of other materials, the present hystereses exhibit a high reproducibility and a large on/off ratio.

Figure 3 shows the current time (*I-t*) characteristics at $|V_{dc}|=1$ V after each application of $|V_{dc}|=2$ V, which are successively obtained after several reproducible *I-t* characteristics were measured. In both heterostructures, the resistance modulation decreases monotonically with time. The retention time of the memory is approximately 10^3 s and is dependent on the duration of V_{dc}.[11] These two observations favor the view that the resistance modulation by V_{dc} is caused mainly by the carrier trapping/detrapping at the interface as suggested in Ref. 11. Here, the change of the TFL/PFL onset voltage can explain a sharp I_L modulation.

To minimize the effect of carrier trapping/detrapping, we attempt to modulate the resistance by a short V_{pulse} (0.1–1 ms). No resistance modulation by V_{pulse} is observed at a low V_{dc} in PLZT/LCO as shown in *IV* and *I-t* characteristics (Fig. 4). By applying V_{pulse}, the *IV* characteristics become noisy and exhibit a hint of modulation. Namely, a $+5$ V 1 ms V_{pulse} *decreases* I_L for $V_{dc}<-1$V [inset of Fig. 4(a)]. A $+10$ V 1 ms V_{pulse} tends to *increase* I_L for $V_{dc}<-1$V, and the *IV* becomes even noisier (Appendix B).

On the other hand, PLZT/STON exhibits evidently a resistance modulation by a V_{pulse}. Resistance is reduced by a $+10$ V 1 ms V_{pulse} and is enhanced by a -10 V 1 ms V_{pulse} [Fig. 5(a)]. However, it is not returned to an original value, presumably because 10 V 1 ms V_{pulse} is too strong for the PLZT/STON. Therefore we used another PLZT/STON for

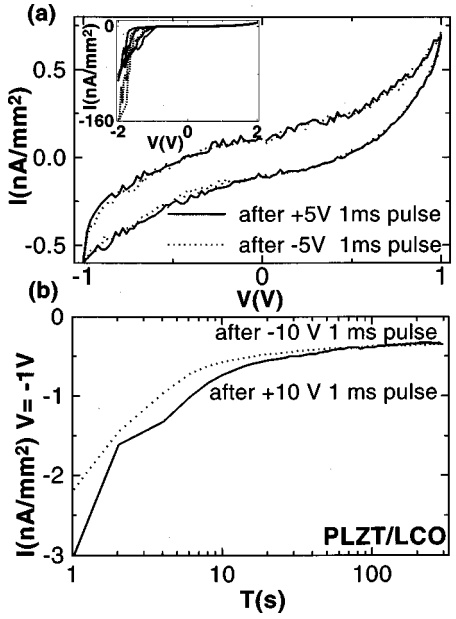

FIG. 4. *IV* curves of Au/PLZT/LCO measured after application of 1 ms V_{pulse}'s of +5 V (——) and −5 V (. . . . .) (main figure: $V_{\max}=1$ V, inset: $V_{\max}=2$ V) (a) and *I-t* curves measured after application of 1 ms V_{pulse}'s of +10 V (——) and −10 V (. . . . .) (b). The sample is that used in Figs. 1(d)–1(f). No pulse resistance modulation is evident except for the noisy result in the inset of (a).

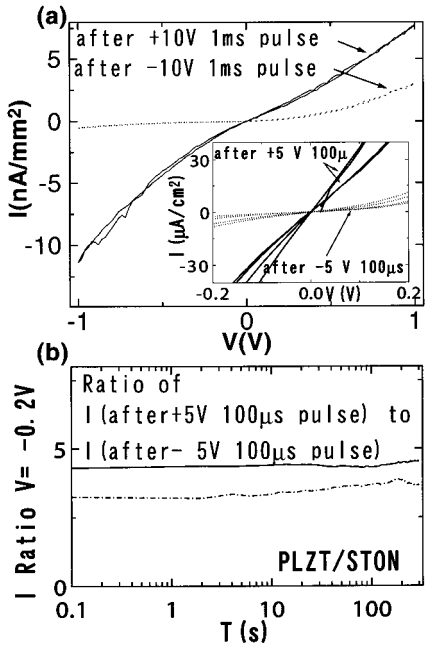

FIG. 5. *IV* curves of Au/PLZT/STO measured after application of 1 ms V_{pulse}'s of +10 V (——) and −10 V (. . . . .) (main figure) and 100 μs V_{pulse}'s of +5 V (——) and −5 V (. . . . .) (inset) (a). The ratio of the current density of *I-t* measured after the application of 100 μs V_{pulse}'s of ±5 V (b). The lines (——) and (—.—.—.—) correspond to the ratio of the second $I(t)$ to the third and, the ratio of the fourth $I(t)$ to the fifth. The sample for the main figure of (a) is that used in Figs. 1(a)–1(c), while the sample of the inset and (b) is different. Pulse resistance modulations are evident.

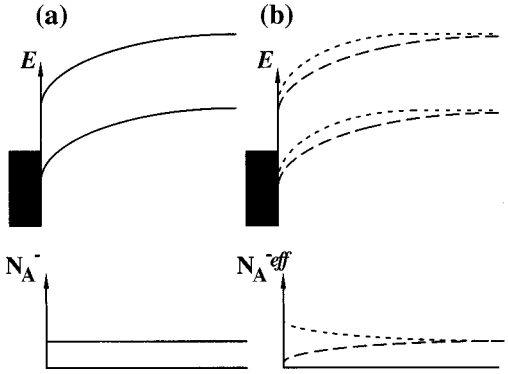

FIG. 6. Band bending by ∇P at $V_{\text{dc}}=0$ and its mathematical equivalence for metal (with shade)/*p*-type ferroelectric with (b) and without the ∇P effect (a). The corresponding effective ionized acceptor density ($N_A^{-\text{eff}}$) is shown below each band diagram, assuming a homogeneous N_A^- distribution and $|P|_{\text{surface}}<|P|_{\text{inside}}$. In (b), the dashed and dotted lines correspond to $P>0$ ($V_{\text{pulse}}<0$ at the metal) and $P<0$ ($V_{\text{pulse}}>0$ at the metal), respectively. Hence the depletion layer is wider for $P>0$ than $P<0$.

the same measurements. The V_{pulse} of +5 V, −5 V, +5 V, and −5 V are successively applied, and the *IV* characteristics are measured after each pulse. The first positive V_{pulse} reduces the resistance drastically [inset of Fig. 5(b)], and the subsequent negative V_{pulse} enhances the resistance but does not also return it to an original value. After the *IV* measurements, *I-t* characteristics are measured by applying +5 V, −5 V, +5 V, and −5 V pulses successively. The resistance modulation persists for a long time [Fig. 5(b)] in contrast with the dc voltage induced modulation. The resistance is found to increase slowly with time even without application of V_{pulse}, which, we think, is responsible for the incomplete reproducibility in Fig. 5(b). Very reproducible pulse switching having a long retention, e.g., 24 hours, is obtained using a $Pb(Zr,Ti)O_3$/STON (Appendix B).

IV. BAND BENDING BY *P*

The current through a ferroelectric is partly controlled by its band bending. The band bending is changed (I) by the depolarization field in the ferroelectric E_f, (II) by the surface states, (III) by the charge distribution, and (IV) by the work function. Few experimental evidences for the work function change by *P* are reported so far.

The origin of E_f is an effective separation of the bound charges due to *P* from the shielding charges, i.e., an imperfect screening of *P*. Such a separation is realized (Ia) by the ∇P effect (Fig. 6),[14] (Ib) by the contact of the ferroelectric surface with an insulator or a semiconductor,[23,4] and (Ic) by the degradation of the ferroelectric surface, i.e., formation of an extraneous surface dead layer during the sample preparation.[24]

The $\nabla P\neq 0$ effect (Ia) is equivalent to the bound charge distribution $P'\delta(x)+\delta P(x)/\delta x$ [$x=0$ is the ferroelectric surface and $|P'|\neq|P|$]. Therefore the bound charges $\delta P(x)/\delta x$ are separated from the shielding charges in the electrode. Alternatively, the effective charge concentration for $x>0$ is expressed by $\varepsilon\varepsilon_0\nabla\cdot E_f=\rho-\nabla\cdot P=\rho-\delta P(x)/\delta x$ using $\nabla\cdot D=\rho$ and $D=\varepsilon\varepsilon_0 E_f+P$. Therefore the switching of *P* changes the effective charge concentration

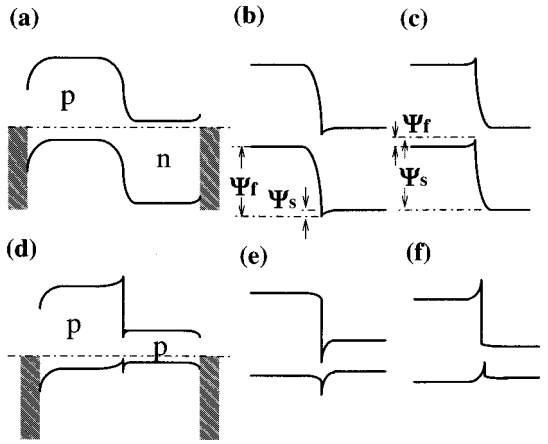

FIG. 7. Approximate band diagrams for metal/PLZT/STON (a)–(c) and metal/PLZT/LCO (d)–(f). The band offsets are assumed to be zero. The figures (a) and (d), (b) and (e), and (c) and (f) correspond to $Q=0$, $Q>0$, $Q<0$, respectively, where Q is the sheet bound charge density at the PLZT/semiconductor interface. If Q is due to P, $Q<0$ is expected in as-deposited sample owing to the builtin potential. (Q can also be due the surface states.)

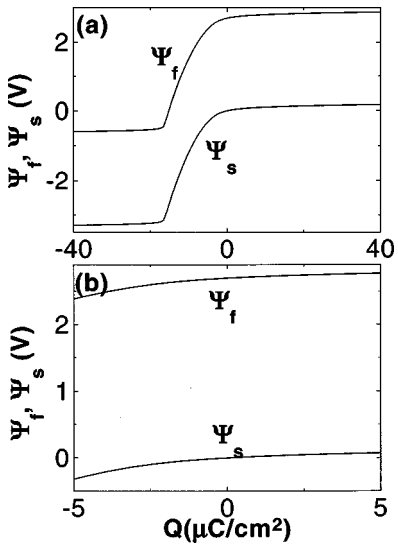

FIG. 8. Builtin potential vs interface bound charge Q at 25 °C for no external field in PLZT/STON calculated according to the procedures described in Ref. 4. The parameters used in the calculation are donor density in STON: 10^{19} cm^{-3}, acceptor density in STON: 0, donor density in PLZT: 0, acceptor density in PLZT: 10^{18} cm^{-3}. Band gaps of PLZT and STON: 3.2 eV, built-in potential for $Q=0$; -2.7 V with no interfacial states assumed. Ψ_s and Ψ_f are defined in Fig. 7.

and, hence, the band bending (Fig. 6).

The effect of the contact of P with an insulator (Ib) or the effect of an insulating surface dead layer (Ic) is estimated for a ferroelectric with a thickness l having a nonferroelectric insulator with a thickness l_d and a dielectric constant ε_i. The electric flux in the insulator D_i is related with E_f by $D_i = -\varepsilon\varepsilon_0 E_f + P$ and the continuity of the potential $E_f l = D_i l_d/\varepsilon_i\varepsilon_0$, yielding $E_f = P l_d/\varepsilon_i\varepsilon_0(l + l_d\varepsilon/\varepsilon_i)$. The nonzero E_f bends the band.

When a ferroelectric is contacting with a nonferroelectric semiconductor (Ib) or the dead layer is semiconducting (Ic), the P switching can also change the band bending. The switching of P by $V_{\text{pulse}}>0$ can change the band diagram from Fig. 7(c) to Fig. 7(b) or Fig. 7(a), which corresponds to decrease of the barrier height $\delta\phi$ for electrons.[25] Experimentally, the band bending of a semiconductor electrode by P is supported by a ferroelectric field effect.[26] Figure 8 shows a calculated potential change of PLZT on STON by the effective P (P_{eff}) [$P_{\text{eff}} = P(A^+ - A^-)$, A^+: area of $+P$ domain, A^-: area of $-P$ domain].

If the thickness of the region of $\nabla P \neq 0$ is much shorter than l, the P distribution and E_f are well approximated by those in a ferroelectric with a surface dead layer.[24,4] Furthermore, a weakly damaged layer formed through the interdiffusion of electrode material can produce a ferroelectric layer of $\nabla P \neq 0$. Therefore an apparent ∇P effect can easily be created during the sample preparation. Examples of the problems are the change of the chemical composition near the ferroelectric surface, the reaction of the surface with the moisture, the defects near the surface, and the reaction of the surface with the electrodes that occur easily during electrode annealing. This is the reason why we did not perform the post annealing of the samples after electrode deposition.

A charge injection into the semiconductor surface region is known to change the surface states (II) and the charge distribution (III). Additionally, excessive surface states (II) may change the Schottky barrier height (IV). The surface states formation inside the ferroelectric (II) is equivalent to doping and reduces the depletion layer width W. [$W \propto N_{D+}^{1/2}(N_{A^-}^{1/2})$, $N_D(N_A)$: donor (acceptor) density.] Therefore the effect of the charge injection on W is similar to the ∇P effect, although the dependence of W on the polarity of the applied voltage is expected to be opposite if $|P'|<|P|$ (Fig. 6). Similarly, the charge redistribution in the ferroelectric (III) can increase and decrease W.

V. DISCUSSION

A. Origin of resistance modulation

First, Fig. 2(f) shows that reverse biased Schottky barrier exhibits only relaxation. This suggests the reason why few papers report the resistance modulation in the metal/ferroelectric(dielectric)/metal (MFM). Namely, in the MFM, I_L is always limited by a reverse biased Schottky barrier. On the other hand, both PLZT/*n*-type semiconductor and PLZT/*p*-type semiconductor heterostructures exhibit the resistance modulation *at forward bias*.

As mentioned in Sec. III, the dependence of the current density on the top metal electrode material and the dependence of the forward polarity on the bottom semiconductor verify that the I_L is mainly limited at the metal/PLZT interface in metal/PLZT/LCO and at the PLZT/STON interface in metal/PLZT/STON. This is explained by a band diagram in Fig. 7.

The modulation by V_{dc} and its loss are explicable by the P switching, or the charge injection, or the charge redistribution. For the latter two causes, the relatively long retention time is likely achieved by an extraordinarily slow relaxation rate. Indeed, a similar resistance modulation is found to increase with temperature and exist even above its Curie temperature in Au/$BaTiO_3$/STON.

Blom *et al.* reported *IV* characteristics similar to Fig. 1(f) in Au/$PbTiO_3$(200 nm thick)/$La_{0.5}Sr_{0.5}CoO_3$ (*p*-type conductor).[12] Furthermore, they observed a persistent modulation by V_{dc} of ± 10 *V*. However, only one cycle of an *IV* curve and one resistance measurement of a high and a low resistance state are shown, and no reproducibility is addressed. Assuming a ∇P effect, it was attributed to the change of the band bending near the Schottky barrier by the *P* switching. The poling process, i.e., the application of a large electric field to align *P*, is known to be a complex process which redistributes also the charges and traps near the surface.[27] Judging from the *IV* characteristics, the current of an enormous density is expected to flow at ± 10 V, which creates a possibility that a small fraction of the carriers were injected and remained trapped for a long time.

The results of Ref. 12 is to be compared with our results for PLZT [or (Pb,La)TiO_3, $Pb(Zr,Ti)O_3$]/LCO, because both $La_{0.5}Sr_{0.5}CoO_3$ and LCO are *p*-type. In this case, they and we think that metal/ferroelectric interface regulates I_L. First, we observed *IV* characteristics very similar to theirs at V_{dc} much lower than the coercive field of the sample (Au/$PbZr_{0.2}Ti_{0.8}O_3$/LCO). However, the *IV* curves were irreproducible in the repeated measurement, which is a common problem in the measurement of the diode current. Furthermore, as shown in Fig. 4, V_{pulse} switching was observed. However, the *IV* exhibited an extraneous features similar to those of Ref. 12 and has an insufficient reproducibility. In the present paper, the current density is lower by an order of 3 to 4 ($\geqslant 4$ for poling) than that of Ref. 12 and the samples retained an original high impedance showing reproducible *IV* after many runs. We think that these differences are the reason why we observed no persistent modulation by V_{dc} in metal/PLZT/LCO. Because we are concerned with the reproducibility and the quality of the *IV* curves, we conclude that a *P*-induced modulation is hardly observed in metal/PLZT/*p*-type semiconductor.

On the other hand, the injection is suppressed by use of the short pulse. Figure 5 demonstrates that the V_{pulse} resistance modulation is repeated and retained for a long time in Au/PLZT/STON. The modulation is likely attributable to the *P* switching. It is true that we could not restore the resistance of Au/PLZT/STON to an initial value by a V_{pulse}, which creates a suspicion that the *p-n* junction was destroyed. However, it is presumably due to the difficulty of the *P* switching caused by the induced low resistance. Indeed, this problem is overcome in other experiments (Appendix B).

Theoretically, the resistance of the Au/PLZT/STON is expected to be tuned by *P* even without a surface dead layer or a ∇P effect (Sec. IV). This is because I_L is limited by a ferroelectric (PLZT)/semiconductor(STON) *p-n* junction. The $\delta\phi$ value at the PLZT/STON is approximately 150 meV for the hysteresis in Fig. 1(c), 250 meV for the transition from Fig. 1(b) to Fig. 5(a), 100 meV for the transition from a low to a high resistance in Fig. 5(a). Figure 8 indicates that these values correspond to change of Q (δQ)$=20$ μC/cm^2 for an initial Q (Q_0)≈ -40 μC/cm^2, $\delta Q \approx 2$ μC/cm^2 for $Q_0 \approx -20$ μC/cm^2, and $\delta Q \approx 10$ μC/cm^2 for $Q_0 \approx 0$. Therefore $\delta\phi$ for the modulation in Fig. 5 lies in the range explicable by the *P* switching. The absence of the pulse modulation in metal/PLZT/LCO suggests that the effects of ∇P and a dead layer are negligible.

B. Implication for ferroelectric field effect transistor (FET)

The metal/ferroelectric/semiconductor (FS) and the metal/ferroelectric/insulator/semiconductor (FIS) structures are intensively studied to realize a ferroelectric FET. Although a long retention of the transconductance modulation is reported,[26] it is lost in minutes or hours in most studies. This time scale for retention agrees with that of the dc modulation of *IV*, suggesting its relevance. Indeed, it is well known that the transconductance is modulated by carriers injected from the semiconductor in FS.[28] Additionally, there is a possibility for the carriers injected from the metal contact to modulate the transconductance in FIS.

C. Conduction mechanism, relaxation, and diode polarity

The conduction mechanisms in perovskite dielectrics and ferroelectrics have been attributed to SCL,[29] TEL,[30,31] or PFL.[30] For example, the electrode dependence of I_L supports a TEL, the *IV* plots support a SCL, or sometimes a PFL, or a TEL at a high V_{dc}. Here, the SCL and the PFL are regarded as bulk transport processes, while the TFL is regarded as an electrode limited transport process.[30] The different conduction mechanisms ascribed by the previous reports can be consistently explained by the depletion layer. Here, an extraordinarily low polaron mobility in PLZT seems responsible for the appearance of the SCL conduction that is rarely observed in the current through the depletion layer of the conventional semiconductors.

First, below $|V_{dc}| \leqslant 1$V, the *IV* characteristics are symmetric to V_{dc} [Figs. 1(b) and 1(f)]. Additionally, an appreciable fraction of I_L is due to a relaxation, and the *IV* characteristics are fitted well with a SCL model that is pertinent to an insulator which has no free carriers. However, the free carriers are abundant in the bulk part of PLZT and STON.[32] Moreover, the *IV* characteristics limited by the electrode exhibit also the SCL [Figs. 2(b) and 2(e)]. These contradictions are solved, if we assume the SCL conduction in the depletion layer of the Schottky contact or the *p-n* junction. By assuming the trapping/detrapping process in the depletion layer, the model accounts for the relaxation.[33] If this interpretation of the relaxation is correct, the relaxation is expected to be prominent as the builtin potential or the reverse bias increases, because the depletion layer widens. Indeed, Dietz *et al.* found that the relaxation becomes evident as the Schottky barrier increases.[31] On the contrary, the dielectric relaxation,[34] which is frequently assigned to the relaxation as in Fig. 1, cannot explain the extraordinarily slow relaxation rate [$I_L \propto t^{-n}$ $(0.2 < n \leqslant 1)$] and the apparent SCL conduction.[30,35]

When $|V_{dc}|$ is increased, the carriers in the space charge layer are slowly emitted and are redistributed, e.g., from Fig. 9(b) to 9(a). The polarity of the resulting current inside the PLZT is the same as V_{dc}. When $|V_{dc}|$is reduced, the carriers return to the initial positions as seen for the change from Fig. 9(a) to 9(b). The polarity of the resulting current inside the PLZT is opposite to V_{dc} for $0 < V_{dc} < V_{max}$. We should note that I_L can flow in the circuit without the carrier transport across the Schottky barrier (or *p-n* junction). Namely, due to an image charge effect, the carrier redistribution in the PLZT depletion layer changes the carrier concentration in the electrode and yields I_L in the measurement system. Therefore the

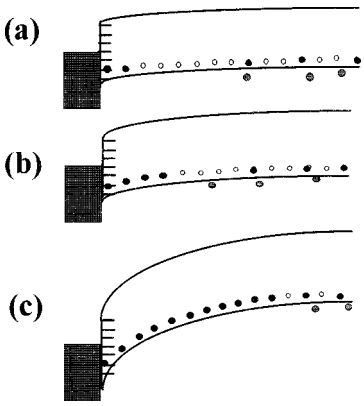

FIG. 9. Band bending of PLZT by an external bias and the trapping/detrapping for a forward bias (a), zero bias (b), a reverse bias (c). The filled circles, the open circles, and the half filled circles show the ionized acceptors, the acceptors trapping a hole, and the holes, respectively.

carrier redistribution inside the PLZT during the band bending can explain the relaxation current. Accordingly, the apparent conduction mechanism is a bulk limited transport such as PFE and a SCL as observed in Figs. 2(a) and 2(d).

As V_{dc} increases, a substantial fraction of I_L is expected to flow across the metal/PLZT interface,[36] and IV characteristics asymmetric to V_{dc} emerge. If I_L is limited by the barrier of a sharp metal/PLZT contact having a high work function metal, the TEL characteristics are expected. Otherwise, the SCL or the PFL in the PLZT depletion layer is expected. In this process, the holes are emitted from traps in PLZT, yielding a net increase of N_{A^-} in PLZT, which is likely related with the memory effect.

The preceding discussions indicate that the diodelike current is limited by the PLZT/STON interface in metal/PLZT/STON and by the metal/PLZT interface in metal/PLZT/LCO. This is consistent with the band diagrams based on the work function difference in Figs. 8(a) and 8(d). According to the literature,[12,30,35,37–40] the top of the valence band of PLZT and LCO, the bottom of the conduction band of STON, and the Fermi levels of Au and Pt are approximately -7 eV, $-5.5\sim-6$, -4, -5, and -5.5 eV from the vacuum level, respectively. Accordingly, the builtin potentials based on the work function difference $\delta\phi$ are -2 V for Au/PLZT, $-1.5\sim-2$ V for PLZT/LCO, -3 V for PLZT/STON (experimental values seem lower than these). Therefore I_L is expected to be controlled by the Au/PLZT interface in Au/PLZT/LCO and by the PLZT/STON interface in Au/PLZT/STON, assuming that the resistance in the bulk part of the PLZT layer is negligible. Indeed, for Au/PLZT/LCO, the observed forward bias polarity corresponds to that of a Schottky contact of p-type semiconductor, and, for Au/PLZT/STON, that of a p-n junction.

VI. CONCLUSION

We have studied IV characteristics of various metal/Pb-based ferroelectrics/n-type and p-type semiconductors of a sufficiently high resistance at RT. At a low V_{dc} the IV are symmetric and relaxation dominated. At a high V_{dc} the IV are diodelike, exhibiting a highly reproducible hysteresis and a well defined sharp threshold for a current jump. The polarity of the forward bias is invariably determined by the conduction type of the semiconductors, i.e., positive for n-type and negative for p-type. The band diagrams based on the work function differences suggest p-n junction for PLZT/STON and p-p for PLZT/LCO. The various experimental results including metal electrode dependence are consistently explained by the diagram, and I_L is limited by the p-n junction in the metal/PLZT/STON and by the metal/PLZT contact in the metal/PLZT/LCO.

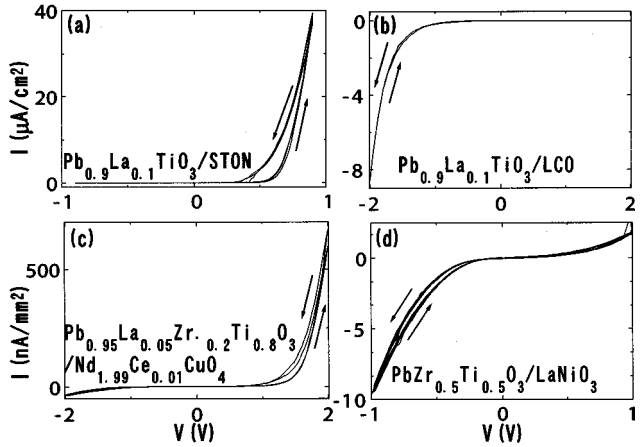

FIG. 10. IV curves of $Pb_{0.9}La_{0.1}TiO_{3\pm\delta}$/STON (a), $Pb_{0.9}La_{0.1}TiO_{3\pm\delta}$/LCO (b), $Pb_{0.95}La_{0.05}Zr_{0.2}Ti_{0.8}O_{3\pm\delta}$/NCO (c), and $PbZr_{0.5}Ti_{0.5}O_{3\pm\delta}/LaNiO_3$ (d). Panels (a)–(d) exhibit three, one, two, and five IV curves consecutively measured, respectively. The diode polarities are consistent with Fig. 1. STON and NCO are n type, and LCo and $LaNiO_3$ are p type.

In both PLZT/STON and PLZT/LCO structures, the application of a forward $|V_{dc}|$ of 2–4 V induces a reproducible resistance modulation decreasing with time. However, a reproducible resistance modulation by a V_{pulse}, which is an important criterion for identifying a P induced modulation, is possible only in the PLZT/STON. The resistance modulation by a V_{dc} is attributed to the carrier injection into the PLZT surfaces and its unusually slow relaxation that may be related with the electron-lattice coupling in the ferroelectric. Nonetheless, the carrier injection may indirectly affect P switching, because the pinning of P at surface is possibly changed by this process.

Theoretical calculation indicates that a small P switching can modulate the resistance, when the resistance regulated by

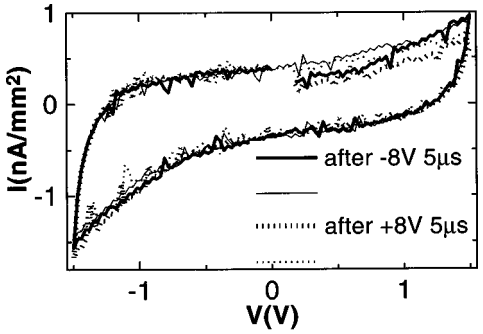

FIG. 11. IV curves of $Pt/Pb_{0.95}La_{0.05}Zr_{0.5}Ti_{0.5}O_{3\pm\delta}$/Pt after the V_{pulse} application. The thick and thin lines show two IV curves measured after each V_{pulse}. No pulse resistance modulation is evident.

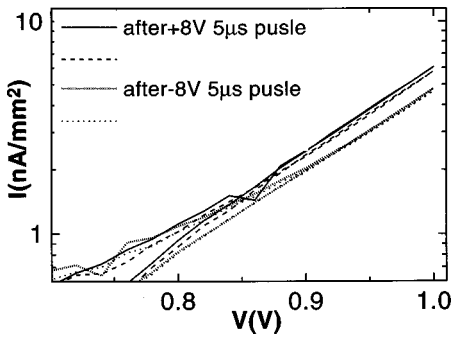

FIG. 12. *IV* curves of $Au/Pb_{0.95}La_{0.05}Zr_{0.2}Ti_{0.8}O_{3\pm d}$/STON after the V_{pulse} application. Four lines show *IV* measured 7 min after the successive application of V_{pulse}'s of +8 V (——), −8 V (. . .), +8 V (— — —), and −8 V (. . .). Each *IV* is identical to the *IV* measured immediately after the V_{pulse} application that is not shown. Recurrent pulse resistance modulations and the high reproducibility are evident.

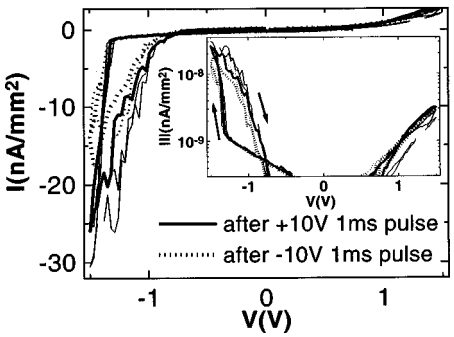

FIG. 13. *IV* curves of Au/PLZT/LCO measured after the V_{pulse} application of +10 V (——) and −10 V (. . .). Inset is a replot in logarithmic scale. The five curves correspond to *IV* after the successive application of V_{pulse}'s of +10 V, −10 V, +10 V, −10 V, and +10 V. Pulse modulations having noisy *IV* characteristics with an insufficient reproducibility are only seen. No modulations are seen at all for lower V_{pulse} or shorter pulse width.

a semiconductor/ferroelectric junction like PLZT/STON. This is regardless of the assumption of an insulating or a semiconducting ferroelectric. When the resistance is regulated by an ideal metal/ferroelectric contact, no modulation is theoretically expected without a special assumption such as $\nabla P \neq 0$. In the present experiments, where a surface dead layer is carefully reduced, it is safer to conclude that the modulation by P and ∇P are absent at the metal/PLZT.

In the present samples, *IV* characteristics appear to be SCL at a low V_{dc} and SCL or TFL/PFL at a high V_{dc}. A high V_{dc} appears to change the conduction mechanism from a TFL/PFL to a SCL. The *IV* can be explained as a transport in the depletion layer. The relaxation often called as a dielectric relaxation is attributed to the trapping/detrapping of carrier in the process of the band bending.

ACKNOWLEDGMENTS

This work was performed under the support through Grant-in-Aid for Scientific Research from the Ministry of Education, Science, Sports No. 08455014. Y.W. acknowledges Professor S. Uchida for useful discussions and Motochika Okano for the data in a part of Appendix B.

APPENDIX A: MATERIAL DEPENDENCE

Figure 10 shows examples of material dependence.[17,18] A low resistance bottom metal electrode was used, and a high resistance top metal electrode was carefully chosen. A few heterostructures exhibit no resistance modulation up to $|V_{dc}| = 3$ V.

APPENDIX B: V_{pulse} MODULATION OF *IV* IN Pb FERROELECTRICS HAVING VARIOUS COMPOSITIONS (Ref. 41)

The Pb oxide ferroelectric films below are 200–300 nm thick. Polycrystalline $Pt/Pb_{0.95}La_{0.05}Zr_{0.5}Ti_{0.5}O_3$/Ptfilms are prepared by a sol-gel process, whereas all others are epitaxially grown by a laser deposition. The V_{pulse} width and the intensity are determined from the Sawyer-Tower hysteresis measurements and the delay constant of each sample, so as to ensure the P switching and suppress the charge injection simultaneously.

1. $Pt/Pb_{0.95}La_{0.05}Zr_{0.5}Ti_{0.5}O_3/Pt$

Saturated well-defined hystereses are observed at ac voltage (V_{ac}) of 9 V at 50 kHz, and Pr is approximately ±12 $\mu C/cm^2$ at 50 kHz and ±10 $\mu C/cm^2$ at 100 kHz. The first 5 μs V_{pulse} of −6 V reduced slightly the relaxation current. However, the subsequent 5 μs V_{pulse}'s of ±6 V induced no change of *IV*. Similarly, the first 5 μs V_{pulse} of −8 V reduced slightly the relaxation current, but the subsequent 5 μs V_{pulse}'s of ±8 V induced no change (Fig. 11). Some samples break down for 5 μs V_{pulse} of 8 V. These results suggest no V_{pulse} modulation in this heterostructure.

2. $Au/Pb_{0.95}La_{0.05}Zr_{0.2}Ti_{0.8}O_3$/STON

Unsaturated hystereses with Pr of ±3 $\mu C/cm^2$ are observed at V_{ac} of 8 V at 100 kHz. A highly reproducible pulse modulation of the resistance is observed in agreement with the result for PLZT/STON in the text. A +8 V 5 μs V_{pulse} decreases the resistance, and a −8 V 5 μs V_{pulse} increases it (Fig. 12). The modulation is retained at least for a day. Similar results are obtained for $Au/PbZr_{0.2}Ti_{0.8}O_3$/STON, although the reproducibility was insufficient.

3. $Au/Pb_{0.95}La_{0.05}TiO_3$/LCO, Au/PLZT/LCO

Unsaturated hystereses with Pr of ±4 $\mu C/cm^2$ are observed at V_{ac} of 8 V at 20 kHz. A pulse modulation of the resistance having an acceptable reproducibility was observed. A −8 V 100 μs V_{pulse} decreases the resistance, and a +8 V 100 μs V_{pulse} increase it. The modulation was lost after 8 h, and the polarity of the increasing resistance is opposite to that for the ∇P effect.

When a 100 μs V_{pulse} of ±8 V is applied to the Au/PLZT/LCO used for Figs. 1–4, the resistance modulation is vaguely seen as in Fig. 13. The polarity of the increasing resistance agrees with that for the ∇P effect. The noisy irreproducible *IV* is insufficient to support a ∇P induced modulation. No reproducible resistance modulation is observed for $Au/PrZr_{0.2}Ti_{0.8}O_3$/LCO.

[1] K. Kristoffel and P. Konsin, Ferroelectrics **6**, 3 (1973).
[2] W. Känzig, Phys. Rev. **98**, 549 (1955); W. J. Merz, J. Appl. Phys. **27**, 938 (1956).
[3] R. E. Cohen, Ferroelectrics **194**, 323 (1997).
[4] Y. Watanabe, Phys. Rev. B **57**, 789 (1998); J. Appl. Phys. **83**, 2179 (1998); **84**, E3428 (1998).
[5] G. G. Harman, Phys. Rev. **111**, 27 (1958); M. E. Drougard, H. L. Funk, and D. R. Young, J. Appl. Phys. **25**, 1166 (1954); A. G. Chynowerth, Phys. Rev. **102**, 705 (1956); S. Triebwasser, *ibid*. **118**, 100 (1960); V. M. Friedkin, A. A. Grekov, N. A. Kosonogov, and T. R. Volk, Ferroelectrics **4**, 169 (1972).
[6] V. M. Fridkin, *Ferroelectric Semiconductors* (Plenum, New York, 1980) (especially, Chap. 6 for summary of experimental results).
[7] W. Schottky, Naturwissenschaften **26**, 843 (1938).
[8] N. F. Mott, Proc. Cambridge Philos. Soc. **34**, 568 (1938); W. Schottky, Phys. Z. **41**, 570 (1940).
[9] A. G. Milne and F. L. Feucht, *Heterojunction and Metal Semiconductor Junction* (Academic, New York, 1972).
[10] Y. Watanabe, Y. Matsumoto, M. Tanamura, H. Asami, and A. Kato, Physica C **235-240**, 579 (1994).
[11] Y. Watanabe, Appl. Phys. Lett. **66**, 28 (1995).
[12] P. Blom, R. Wolf, J. Cillessen, and M. Krijn, Phys. Rev. Lett. **73**, 2107 (1994).
[13] K. Gotoh, H. Tamura, H. Takeuchi, and A. Yoshida, Jpn. J. Appl. Phys., Part 1 **35**, 39 (1996).
[14] W. R. Kretschmer and K. Binder, Phys. Rev. B **20**, 1065 (1979); D. R. Tilley and B. Zeks, Solid State Commun. **49**, 823 (1984).
[15] Y. Watanabe, Phys. Rev. B **57**, R5563 (1998).
[16] We have chosen this composition because it showed a high reproducibility for 50 cycles of write/read. In a bulk form, the composition $Pb_{1-y}La_yZr_{1-x}Ti_xO_3$ with $x=0.3$ and $y=0.1$ usually corresponds to a relaxor [G. A. Smolensky, V. A. Isupov, A. I. Agranovskaya, and S. N. Popov, Sov. Phys. Solid State **2**, 2584 (1961), L. E. Cross, Ferroelectrics **76**, 241 (1987)]. However, the relaxor behavior is rarely observed in thin film $Pb_{1-y}La_yZr_{1-x}Ti_xO_3$ with $x \leqslant 0.3$ and $y \leqslant 0.1$. Indeed, $Pb_{1-y}La_yZr_{1-x}Ti_xO_3$ epitaxial films with $y \leqslant 0.1$ is frequently reported for the study of the ferroelectric properties. Here, La is doped to increase the resistance of the thin film.
[17] Y. Watanabe, M. Tanamura, Y. Matsumoto, H. Asami, and A. Kato, Appl. Phys. Lett. **66**, 299 (1995).
[18] The relatively low Pr is not due to the relaxor behavior or to the quality of the sample because of the following reasons: (1) The *Pr/Ps* ratio (0.2) is acceptable as that of a ferroelectric film (Ps: the maximum polarization in the hysteresis). (2) The shapes of hysteresis are almost the same for PLZT in the range of $y=0-0.1$ and also for $BaTiO_3$. Pr of $BaTiO_3$ is as low as 1 $\mu C/cm^2$ but this value is a relatively good value as 200-nm-thick $BaTiO_3$ film. (3) The relatively low Pr is due partly to a unsaturated hysteresis caused by a high coercive field Ec in epitaxial films. We did not perform annealing of the metal electrode and post annealing of the ferroelectric films to avoid creating an artificial ∇P effect. This increases Ec further and reduces the effective contact area of the metal electrode. Therefore the real Pr is not as low as stated in the text.
[19] Y. Watanabe, D. Sawamura, and M. Okano, Appl. Phys. Lett. **72**, 2415 (1998).
[20] M. Okano, D. Sawamura, and Y. Watanabe, Jpn. J. Appl. Phys., Part 1 **37**, 5101 (1998).
[21] The same polarity dependence on the semiconductor is found in Au(Al,Pt)/$BaTiO_3$/STON, Au(Al,Pt)/$BaTiO_3$/LCO, Au/$Bi_4Ti_3O_{12}$/STON, and Au/$Bi_4Ti_3O_{12}$/LCO (Ref. 21). Although $BaTiO_3$ is reported to be *n* type, the polarity dependence is explicable consistently with the present results for Pb-Ti based ferroelectrics. Y. Watanabe, D. Sawamura, and M. Okano, Appl. Surf. Sci. **130-132**, 682 (1998); Solid State Ionics **108**, 109 (1998); J. Korean Phys. Soc. **32**, S1361 (1998); Y. Watanabe, Y. Matsumoto, and M. Tanamura, Jpn. J. Appl. Phys., Part 1 **35**, 5745 (1996).
[22] K. C. Kao and W. Hwang, *Electrical Transport in Solids* (Pergamon, Oxford, 1981); N. F. Mott and R. W. Gurney, *Electronic Processes in Ionic Crystals* (Dover, New York, 1940); A. Many and G. Rakavy, Phys. Rev. **126**, 1980 (1962); A. Rose, *ibid*. **97**, 1538 (1955); E. H. Snow, A. S. Grove, B. E. Deal, and C. T. Sah, J. Appl. Phys. **36**, 1664 (1965); H. H. Poole, Philos. Mag. **32**, 112 (1916); J. Frenkel, Phys. Rev. **54**, 647 (1938).
[23] P. Wurfel and I. P. Batra, Phys. Rev. B **8**, 5126 (1973).
[24] Y. Watanabe and A. Masuda, Ferroelectrics **217**, 53 (1998).
[25] The current regulation is ascribed to the Au/PLZT interface in Au/PLZT/LCO interface and the PLZT/STON interface in Au/PLZT/STON in the text. However, when the Au/PLZT in Au/PLZT/LCO or the PLZT/STON in Au/PLZT/STON is forward biased, the PLZT/LCO interface in Au/PLZT/LCO or the Au/PLZT in Au/PLZT/STON is reverse biased. Therefore it is also theoretically possible for the PLZT/LCO interface (the Au/PLZT in Au/PLZT/STON) to regulate the current when they are reverse biased, although this possibility is rejected by the dependence of the current density on the metal electrode material. Nonetheless, the possibility can remain for conduction at a very large V_{dc} and may produce a *P* induced resistance modulation in PLZT/LCO, which may be related with a hint of resistance modulation shown in the inset of Fig. 6.
[26] K. Sugibuchi, Y. Kurogi, and N. Endo, J. Appl. Phys. **46**, 2877 (1975); Y. Watanabe, M. Tanamura, and Y. Matsumoto, Jpn. J. Appl. Phys., Part 1 **35**, 1564 (1996); Y. Watanabe, Appl. Phys. Lett. **66**, 1770 (1995).
[27] B. Jaffe, W. Cook, and H. Jaffe, *Piezoelectric Ceramics* (Academic, London, 1971); D. Dimos, W. L. Warren, M. N. Sinclair, B. A. Tuttle, and R. W. Schwartz, J. Appl. Phys. **76**, 4305 (1994); W. L. Warren, H. N. Al-Shareef, D. Dimos, B. A. Tuttle, and G. E. Pike, Appl. Phys. Lett. **68**, 1681 (1996).
[28] S. Y. Wu, IEEE Trans. Electron Devices **21**, 499 (1974).
[29] G. R. Fox and S. B. Krupanidhi, J. Appl. Phys. **74**, 1949 (1993).
[30] C. Sudhama, A. C. Campbell, P. D. Maniar, R. E. Jones, R. Moazzami, C. J. Mogab, and J. C. Lee, J. Appl. Phys. **75**, 1014 (1994).
[31] G. W. Dietz, W. Antpohler, M. Klee, and R. Waser, J. Appl. Phys. **78**, 6113 (1995).
[32] For a tentative value of the mobility of 10^{-8} $cm^2\,V^{-1}\,s^{-1}$ and plausible values of the carrier density of 10^{17} cm^{-3} and the electric field of 10 kV cm^{-1}, the current density is 10 nA mm^{-2} and much larger than the observed current density.
[33] Samples having a low resistance tend generally to exhibit Ohmic conduction and no relaxation at a low field.
[34] H. Fröhlich, *Theory of Dielectrics*, 2nd ed. (Clarendon, Oxford, 1960).
[35] H. M. Chen, J. M. Lan, J. L. Chen, and J. Y. Lee, Appl. Phys. Lett. **69**, 1713 (1996).
[36] This current is not an apparent current, because the current density is too high to explain by the dielectric relaxation or detrapping of the carriers at the interface (Ref. 11). Temperature *(T)*

dependence of the current density at low T is not fitted well with any of the conduction mechanisms mentioned above and indicated the barrier height of 0.5–0.7 eV both for Au/PLZT and PLZT/STON, which is consistent with PFL model. On the other hand, it has the relationship of $\log I_L \propto T^{-1}$ above RT that is consistent with the PFL model but not with the TEL model (the reverse-biased Schottky barrier). Strictly speaking, we measured only the T dependence of $BaTiO_3$ heterostructures at high T.

[37] H. B. Michaelson, J. Appl. Phys. **48**, 4729 (1977).

[38] P. F. Baude, C. Ye, and D. L. Polla, Appl. Phys. Lett. **64**, 2670 (1994); M. Copel, P. R. Duncombe, D. A. Neumayer, T. M. Shaw, and R. M. Tromp, *ibid.* **70**, 3227 (1997).

[39] K. C. Hass, in *Solid State Physics*, edited by H. Ehrenreich and D. Turnbull (Academic Press, New York, 1989), Vol. 42, p. 213.

[40] Our UV electron emission system estimated that the work function of LCO is larger by about 1 eV than that of Ag (4.3 eV) in air. Additionally, the contact resistance of annealed Au/LCO was larger than that of annealed Pt/LCO, suggesting that the work function of LCO is larger than that of Au, possibly, and that of Pt.

[41] M. Okano, Y. Matsushita, and Y. Watanabe (unpublished).